Validation of a Biomechanical Performance Assessment Platform Applying an Inertial-Bpased Biosensor and Axis Vector Computation

Wangdo Kim[1,2] [a], Sean S. Kohles[3,4,5] [b], Emir A. Vela[1,2] [c] and Victor Huayamave[6] [d]

[1]*Ingeniería Mecánica, Universidad de Ingeniería y Tecnología -UTEC, Lima, Peru*
[2]*Research Center in Bioengineering, Ingeniería Mecánica, Universidad de Ingeniería y Tecnología-UTEC, Lima, Peru*
[3]*Kohles Bioengineering, Cape Meares, OR, U.S.A.*
[4]*Division of Biomaterials & Biomechanics, School of Dentistry, and Department of Emergency Medicine, School of Medicine, Oregon Health & Science University, Portland, OR, U.S.A.*
[5]*Department of Human Physiology and Knight Campus for Accelerating Scientific Impact, University of Oregon, Eugene, OR, U.S.A.*
[6]*Department of Mechanical Engineering, Embry-Riddle Aeronautical University, Daytona Beach, FL, U.S.A.*

Abstract: Inertial kinetics and kinematics have substantial influences on human biomechanical function. A new algorithm for IMU-based motion tracking is presented in this work. This study combines recent developments in improved biosensor technology with mainstream motion-tracking hardware to measure the overall performance of human movement based on joint axis-angle representations of limb rotation. This study proposes an alternative approach to representing three-dimensional rotations using a normalized vector around which an identified joint angle defines the overall rotation, rather than a traditional Euler angle approach. Contrast the procedure of Euler angles with the procedure of Axis angle, Euler angles force the body to move along a certain route which it had arbitrarily chosen but which the body had not chosen; in fact, the body would not take any of its routes separately, though it would take all of them together in the most embarrassing manner-goal-directed behavior. But axis angle had no preconceived scheme as to the nature of the movements to be expressed. Although the axis-angle representation requires vector quotient algebra (quaternions) to define rotation, this approach may be preferred for many graphics, vision, and virtual reality software applications. Elbow flexion and extension motion was used to validate the analytical methods. The results suggest that the novel approach could reasonably predict a detailed analysis of axis-angle migration. The described algorithm could play a notable role in the biomechanical analysis of human joints and offers a harbinger of IMU-based biosensors which may assess the control of skilled manipulation.

1 INTRODUCTION

Human motion capture systems, constructed from Inertial Measurement Units (IMUs), have been the subject of recent development and validation. Lapresa et al. (2022) presented the validation of inertial systems using an anthropomorphic robot (Lapresa et al., 2022). These approaches rely on measuring the three-dimensional linear and angular positions and accelerations of subject joints and limbs generated by micro-electromechanical systems (MEMS) such as an IMU. Effectively, an IMU is a localized biosensor accelerometer and gyroscope estimating an object's biomechanical position and orientation. IMUs can be single-point sensors or more complex single-pack arrays when including an additional magnetometer and sensor fusion algorithm, providing more accurate movement data and reduced sensor drift. A common artifact of accelerometer measurements is manifested in velocity and displacement trajectory drift obtained when integrating the raw acceleration record.

[a] https://orcid.org/0000-0003-0527-5129
[b] https://orcid.org/0000-0002-5869-7715
[c] https://orcid.org/0000-0002-9397-2452
[d] https://orcid.org/0000-0003-0837-6849

MEMS-based IMU sensors can be used in computer vision techniques that track the location of a person through a combination of their pose and orientation with applications in robotics, personal navigation, and virtual reality. Furthermore, recent studies confirm IMU sensor applications for human motion analysis, enhancing biomechanics, rehabilitation, ergonomics, and sports assessments (González-Alonso et al., 2021). This research includes refined quantification of human movements and movement classification. These studies concentrate on obtaining the kinematic Identification of a particular activity, which helps identify biomechanical disorders such as disease or injury, as well as longer-term patterns of atypical neuromuscular control. Compact, self-contained systems for the kinematic Identification of human motion, such as that offered by IMUs, are independent of the subject's mobility environment and free of obstructions that may affect optical position sensors (D'Amore, Ciarleglio, & Akin, 2015).

Current swing dynamic performance indices seem to be insufficient to represent the fundamental of golf dynamic performance because full-body models may be easily affected by the rotation of individual anatomical segments (Teu, Kim, Fuss, & Tan, 2006). Recent studies have suggested that the inertia tensor, a physical property whose values are time- and coordinate-independent, may be an important informational invariant haptic perception of which is not influenced by the segment rotations. Previous work addressing the biomechanical performance assessment platform used an optical-based system (Figure 1) and identified the geometric change to a certain axis, such that if the club is rotated around this axis through a determinate angle, the desired movement will be effected. The perception-action dynamic alignment between the inertia of the club and the instantaneous axis was indexed as an influence on the swing phase of the golf training system (Kim, Veloso, Araújo, Machado, et al., 2013). We found that perception and action were more highly correlated with each other in the more skilled player (Figure 2b) compared to the less experienced player (Figure 2a).

The present study describes the characteristics of an IMU wearable sensor platform that provides a critical biomechanical parameter during the assessment of joint disease and injury. Here, the instantaneous axis-angle representation (IAA) of limb function is a vector that is identified as a metric to assist human movement analysis for use in rehabilitation and sports. The estimation of the IAA

and its variant motion is strongly related to the joint's functionality and ligament health (Kim, Araujo, Kohles, Kim, & Alvarez Sanchez, 2020) as well as the overall performance of locomotion perception and motor control (Kim, 2020). Joint kinematics depend on a postural balance or equilibrium, meaning that the components of the resultant moment about the axis of rotation sum to zero. In this work, we confirm the accuracy of IMU-based inverse kinematics and forward kinematics as applied to upper limb movement.
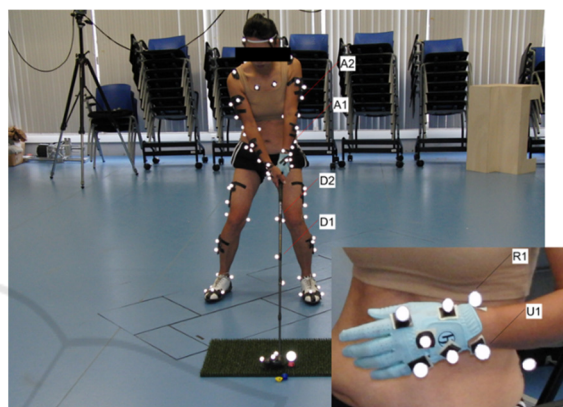

Figure 1: Position of attached markers on the body of the subject that adopted the stance at the instance of the club addressing the ball. The separate panel depicts individual markers attached to the hand. The labeled markers were used to build an anatomical reference frame within which the grip reference frame was coincident at the beginning of the downswing. The origin of the global frame coincides with the first COP location of the left foot.

The specific objective of this work is to present a new algorithm for Inertial measurements unit (IMU)-based motion tracking with quaternions. Axis-angle representation for rotation, instead of representing a 3D rotation using a sequence of rotations around the sensor coordinates system, as Euler angles do, the axis-angle representation uses a normalized vector S around which the rotation is defined by some angle θ and can track a sequence of events in terms of a one-one correspondence of IAA. Although the IAA is not fixed, it is indeed moving about in such an embarrassing manner that has unity relative to the posture and behaviors of the subject being considered.

There are two main advantages to using the axis angle representation for describing limb kinematics. The first is that they allow a global description of rigid body motion that does not suffer from singularities due to local coordinates. Such singularities are inevitable when one represents rotation via Euler
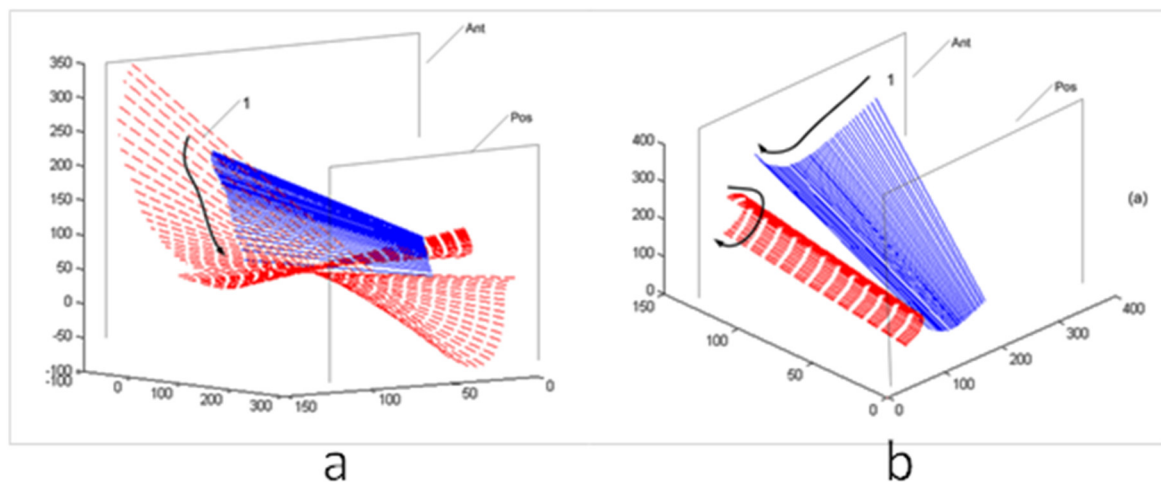
Figure 2: (a), (b). Player A, the novice golf player, produced a three-dimensional spatiotemporal view on the instantaneous axis-angle (IAA, solid lines) and the instantaneous principal axes of inertia (e3, dashed lines) for small motion steps (300Hz) that were projected onto the posteromedial side of the player (a). The endpoints of axes are at the intersections with anterior (Ant) and Posterior (Pos) planes, which are located 100 and 300 cm off the origin of the global frame. The first axis, indicated by 1, represents the beginning of the downswing. The arrow indicates where the subsequent axes have migrated at every 0.0333 second of time step (units in cm).

Player B, the skilled player, produced a three-dimensional spatiotemporal view on the instantaneous axis-angle (IAA, solid lines) and the instantaneous principal axes of inertia (e3, dashed lines) for small motion step (300Hz) that were projected onto the posteromedial side of the player (a) and onto the superior side of the player (b). In an effort to verify positioning perception and action relation in time-sequence of motion data, the club IAA is shown to be regularly projective to the e3. This representative analysis indicates a close connection (Spatial-temporal representation of IAA versus the e3) during the downswing for player B.

angles. The second advantage is that the axis-angle provides a very geometric description of rigid motion, which significantly simplifies the analysis of biomechanisms and is handy for describing the kinesthesis, "feeling of movement," in all skeletal and muscle structures. The axis vector is not moving instantaneously, occupying a stationary axis in the global frames.

2 MATERIAL AND METHODS

2.1 Inertial Measurement Unit Device and Model Foundation

The newest generation of cost-efficient inertial motion trackers features a lightweight design, wireless connectivity (Bluetooth Low Energy, BLE), and robust sensor fusion algorithms to provide accurate data for human movement applications (DOT Wearable Sensor, Xsens Technologies B.V., Enschede, the Netherlands). Software manipulation tools are provided (Software Development Kit, SDK) to facilitate the customization of mobile applications based on the available output data, thereby allowing

developers to integrate the sensor into a wide range of solutions. Robust algorithms (Strap Down Integration, SDI) and a sensor fusion framework (Xsens Kalman Filter Core, XKF) run onboard the sensor to provide accurate physical orientation estimates and minimize the effects of magnetic distortion (González-Alonso et al., 2021).

The IMUs applied in this work contain MEMS type gyroscopes, accelerometers, and magnetometers. These individual sensor signals are fused through a statistical estimation framework to obtain three-dimensional (3D) limb and joint orientation. The output provided by the three main device components is then fed into the signal processing pipeline. The two main algorithms noted above are run onboard the motion tracking sensor (Schumacher, 2006). The sensors are primarily designed to connect to mobile devices such as smartphones that must be BLE-capable (Figure 3).

Before describing the output data, it is prudent to present the types of reference systems used in this paper. Data shall be expressed in terms of local (Sensor Coordinate System, SCS) and global, earth-fixed (Global Reference Coordinate System, GRCS) coordinate systems. The SCS is a right-handed,
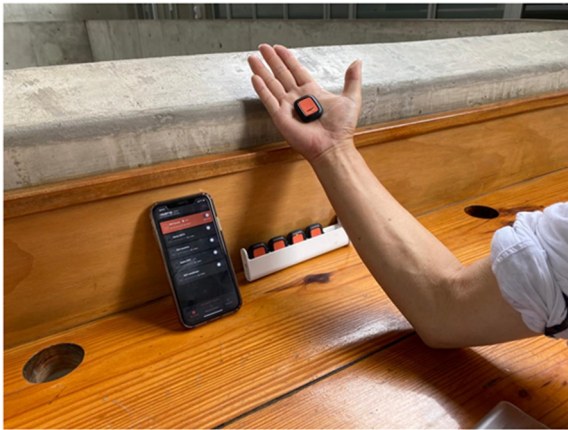
Figure 3: Wireless communication between the sensors and a mobile device was used in this study.

Cartesian coordinate system that is body-fixed within each sensor identified with lowercase x, y, and z axes (Figure 4). The local earth-fixed RC is also defined as a right-handed, Cartesian coordinate system with the following global orientations:

- X positive to the East (E).
- Y positive to the North (N).
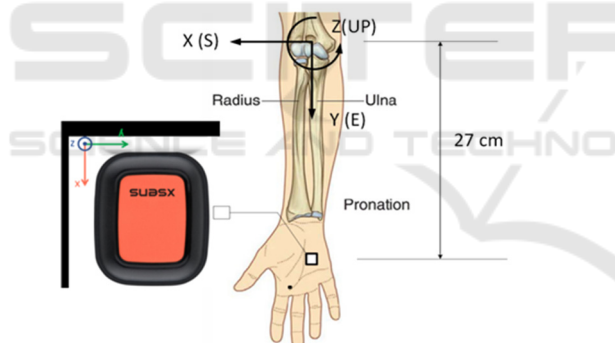- Z positive when pointing Up (U)

Figure 4: The local sensor coordinate system (SCS) is associated with the sensor as indicated by the (x,y,z) Cartesian coordinate system, while the global reference coordinate system (GRCS) is matched to the elbow joint and anatomic orientation as indicated by the (X, Y, Z) Cartesian coordinate system. Since the SCS is not aligned with the GRCS in this anatomic configuration, the data measured by the SCS is transformed through vector algebra by applying the unit quaternion $\left[\cos \frac{\pi}{4}, 0, 0, \sin \frac{\pi}{4}\right]$, which rotates data in SCS by 90 degrees about the Z axis.

This coordinate system is known as East-North-Up (ENU) and is the standard framework in inertial navigation for aviation and geodetic applications. Note that positive global orientations can be established for any application while maintaining the right-hand configuration, i.e., X positive to the South (S).

The wearable sensors produce instantaneous 3D coordinate axis orientation and acceleration data. The data available for the experiment can be classified into two categories: inertial data and sensor fusion data. The inertial data is comprised of linear acceleration (units of m/s^2) and angular velocity (units of °/s) as provided in the SCS. These IMU-based sensors output angular velocities as a direct measurement from the internal gyroscopes. The 3D orientation output takes the quotient of the axis vectors as unit quaternions. The orientation can be represented by a normalized quaternion, q = [W X Y Z] with W being the real component and X, Y, Z as the imaginary global coordinate components. This sensor output is within the ENU localized global reference coordinate system. The output IMU measurement vector S_{raw} contains the individual measurements stacked together as ten state variables:

$$S_{raw} = [a_x, a_y, a_z, \varpi_x, \varpi_y, \varpi_z, q_0, q_1, q_2, q_3] \qquad (1)$$

The optimal filtering problem is then to determine the angular acceleration state variables, $[\alpha_x, \alpha_y, \alpha_z]$ as well as their numerical derivatives as the angular velocity vector components $[\omega_x, \omega_y, \omega_z]$. Further, the problem is then constructing the new state variables, which provide the best match with the data within S_{raw} but also have a degree of numerical smoothness. The regularization method is then applied to solve this numerical challenge (Trujullo & Busby, 1997).

In this study, we estimated the identified state variables by applying L-curve Tikhonov regularization filtering (TRF). The TRF algorithm was previously applied in the optimization of smoothing parameters (Ancillao, Vochten, Verduyn, De Schutter, & Aertbeliën, 2022) during multiscale cell-tissue level (Kim, Tretheway, & Kohles, 2009) and joint level (Kim, Kim, Veloso, & Kohles, 2013) biomechanical analyses. As a result of the TRF, thirteen numerically smoothed state variables are then present in the filtered vector S_{smooth}:

$$S_{smooth} = \begin{bmatrix} a_x, a_y, a_z, \varpi_x, \varpi_y, \varpi_z, q_0, q_1, \\ q_2, q_3, \alpha_1, \alpha_2, \alpha_3 \end{bmatrix} \qquad (2)$$

The data in this application was recorded through local resources (VR Motion Laboratory, Department of Mechanical Engineering, UTEC, Lima, Peru). One healthy, well-trained subject (1 man) gave his written informed consent to participate in this study.

It has frequently been assumed in previous methods that the point of observation for motion is unoccupied because it is measured in a Sensor Coordinate System (SCS), while the point of observation in this work is occupied in global

reference coordinate systems (GRCS.) When a point of observation is occupied, there is also information to specify the motion of himself, and the limb of the person in action instantaneously occupies some portion of the space in a way that is unique to the person as presented as the instantaneous axis-angle representation (IAA.) This information is unique to that person. The IAA is not moving and stationary in the GRCS, occupying the specific axis in the freedom space. Therefore, the innovation brought by this research is to propose the measure of the feeling of the self-movement, i.e., proprioception, in terms of the IAA, meaning that it specifies the self-movement as distinguished from an object moving in the environment.

2.2 Inverse Kinematic Solutions Using Quaternions

Our solution method is based on an axis-angle representation by applying vector algebra quaternions as a motion operator. All rotating screw motions are represented as a rotation about an axis with respect to the global GRCS. Two quaternions describe general movement positioning: one for orientation and the second for translation.

All the data processing was implemented in a commercial programming and computing platform (MATLB, The MathWorks, Natick, MA, USA). Here, the module "Quaternion.m" was applied (Tincknell, 2023). Quaternion.m implements quaternion mathematical operations, including three-dimensional rotations, transformations, and numerical propagation of the governing equations of rotational motion, most of which are fully vectorized.

Quaternions represent complex numbers within a four-dimensional vector space (rank 4) over a real number field (Kuipers, 1999). A quaternion is generalized as

$$q = w + xi + yj + zk = (q_0, q_1, q_2, q_3) \qquad (3)$$

or

$$q = (q_0, \boldsymbol{q_v}) \qquad (4)$$

where q_0 represents a scalar and $\boldsymbol{q_v} = (q_1, q_2, q_3)$ represents a vector. A quaternion of $\boldsymbol{q_v} = 0$ is called a real quaternion, and a quaternion of $\boldsymbol{q_0} = 0$ is identified as a pure quaternion. Multiplication of two quaternion vectors can be expressed as

$$q_a \otimes q_b = q_{a0}q_{b0} - q_{av} \cdot q_{bv}, q_{ao}q_{bv} \qquad (5)$$
$$+ q_{bo}q_{a0} + q_{av} \times q_{bv}$$

where the symbols " $\otimes$ "," $\cdot$ "," $\times$ " denote the quaternion product, dot product, and cross product

actions, respectively. Quaternion multiplication is not considered commutative. The conjugate of the quaternion can be expressed as:

$$q^* = (q_0, -\boldsymbol{q_v}) = (q_0, -q_1, -q_2, -q_3) \qquad (6)$$

and thus defining the quaternion norm $\|q\|$ as:

$$|q|^2 = q \otimes q^* = q_0^2 + q_1^2 + q_2^2 + q_3^2 \qquad (7)$$

With the relationship $\|q\|^2 = 1$, a unit quaternion is present whereby any quaternion (q) can be normalized by dividing by its norm. The inverse of a quaternion is then expressed as:

$$q^{-1} = \frac{1}{|q|^2} q^* \ and \ \|q\| \neq 0 \qquad (8)$$

and thereby for a unit-quaternion, the relationship is reduced to:

$$q^{-1} = q^* \qquad (9)$$

A unit quaternion can be further defined as a vector rotation operator. Rotation about a unit axis ω with an angle θ is then defined by the axis-angle representation (Figure 5).

$$q = \left(\cos\left(\frac{\theta}{2}\right), \sin\left(\frac{\theta}{2}\right)\omega\right) \qquad (10)$$
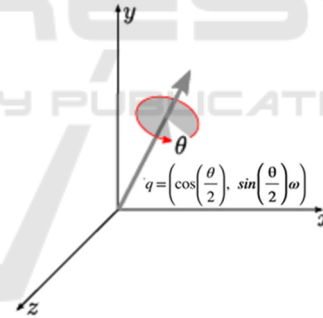

Figure 5: Graphical axis-angle representation for vector rotations. The approach described here uses a normalized quaternion **q** around which the rotation is defined by four kinematic variables instead of three. Applications include computer-aided graphics, vision, and virtual reality computation.

2.3 Biomechanical Orientation Tracking with Quaternions

Earlier work has demonstrated how human perception and motor control interact continuously between external physical systems (Gibson, 1979). The axis-angle representation effectively establishes a global description of the individual as a rigid body during environmental interactions and avoids mathematical singularities due to the use of the local

coordinates. The benefits of using quaternions during axis-angle representation as described in the presented approach are the well-defined sets of operations for vector addition, multiplication, and interpolation while converting the representations directly to rotational matrices. Such singularities are inevitable when representing rotations traditionally via Euler angles.

A general rigid-body transformation has 6 degrees of freedom (DOF) accounting for linear and angular translations or as defined here: 3 DOF for orientation and 3 DOF for translation. A unit-quaternion can be used as a rotation operator as shown in Equation 10 and Figure 3. A vector v can be transformed into a vector w such that:

$$w = q \otimes v \otimes q^* \qquad (11)$$

where q is a unit quaternion and v is a pure quaternion. The unit quaternion can be used to transform a vector, but not through rigid transformation. Therefore, an alternative quaternion will implement translation:

$$t = p - q \otimes p \otimes q^* \qquad (12)$$

Where p is the position vector of an arbitrary point on the axis within a pure quaternion.

In this study, we use the axis-angle representation to obtain the inverse kinematics solution of the elbow during simple flexion and extension within the healthy range of motion of upper limb movement. The immediate objective is to identify the forward kinematics of the hand. For this purpose, it suffices to identify the values of the axis-angle of the elbow joint and its location with respect to the GRCS system. The estimation of the IAA representation of limb movement, also known as a biomechanical screw axis (Ball, 1900), can play a notable role in the biomechanical analysis of biological joints (healthy, diseased, and injured). We assume that the amplitude of the angle of the instantaneous axis is minute, in conformity with a small angle assumption when combined in the same manner as force values.

3 RESULTS

We demonstrate the described IMU-based approach by applying the axis-angle representation of healthy upper limb movements. These experiments: (i) demonstrate the calculation of the IAA and the analysis of IAA migration using quaternion operators; (ii) check the accuracy of both the IMU-based inverse kinematics and forward kinematics. A single male adult subject was used to validate the mathematical approach with data functional anatomic data produced during elbow flexion-extension postures of the upper limb within the sagittal plane of motion. The UTEC human-subjects ethics committee approved the data collection.

The forward kinematics was performed in that sensor trajectories were reconstructed as x,y, z Cartesian coordinates with the help of the IAA. The RC frame was defined for the elbow joint as follows (Figure 4): The origin location is the midpoint of the projection between the medial and lateral bony aspects of the distal humerus. The X-axis defines the lateral aspects of the elbow joint. The X-axis is also coincident with the South (S) orientation according to the ENU global reference coordinate system, the Y-axis is positive to the East (E), and the Z-axis is positive when pointing up (U).

Data were generated by the IMU accelerometer and gyroscope, as provided in the sensor-fixed frame (SCS) and combined through a sensor fusion algorithm measuring the orientation with respect to the global reference frame (GRCS). Therefore, it is necessary to align the SCS frame in which three linear accelerations and three rotational rate gyroscopes are measured to the global coordinates as described above, allowing the IAA to be computed by the global system.

The virtual sagittal plane was defined relative to the geometric representation of the IAA from the geometric center (Figure 6). This allows us to assess variability in the direction of the functional IAA during the flexion-extension movement of the forearm. In addition, the intersection of the functional IAA with this plane was analyzed, while the migration of IAA was observed for small motion steps (acquired at 60 Hz).

Contrast the procedure of Euler angles with the procedure of Axis angle, Euler angles tried to force the body to move along the certain route which it had arbitrarily chosen but which the body had not chosen; in fact, the body would not take any one of its routes separately, though it would take all of them together in the most embarrassing manner—goal-directed behavior. But axis angle had no preconceived scheme as to the nature of the movements to be expressed. A subject simply found the body in a certain position, A, and then he coaxed the body to move, not in this way or in that particular way, but any way the body liked to any new position B.
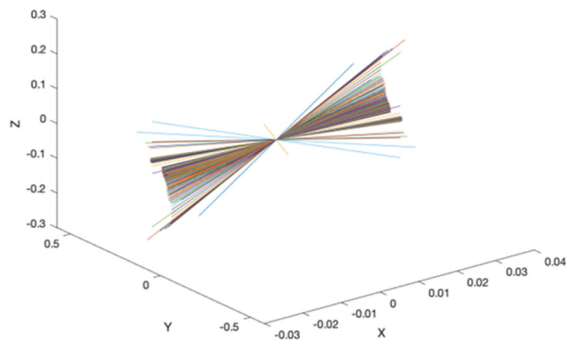
Figure 6: A sequence of IAAs from the single human subject elbow is represented relative to the origin of the global frame (units in meters, m).

Once the IAA was defined, forward kinematics obtained the vector trajectories (Figure 7). Finally, the position of the end effector, the IMU sensor located in the palm of the subject's hand, is given by trajectories as viewed in the oblique and on the sagittal plane.

4 CONCLUSIONS

In theoretical terms, inverse kinematics, which in itself is ruled by an IAA, is formed to visualize the migration of biomechanical action. Another piece of information provided by forward kinematics as ruled by the end effector is formed by visualizing the migration of the motion at the distal or proximal ends of the limb itself. In this way, the characteristics of the elbow motion can be estimated intuitively based on the shape and alignment relative to each of the limb segments. From a mechatronic perspective, we use position and orientation data to control the end effector of a robotic arm. From that application, identifying the joint variables that generate that desired position and orientation will ultimately control the end effector. However, human movement control is continuous and processed concurrently with afferent and efferent inherent modulation.

Limitations of this study are that one IMU sensor was used during the activity of a single subject. The optimal system for joint biomechanics should be characterized using two IMUs where each sensor is worn at the proximal and distal segments containing the target joint. Future research will focus on increasing the use of IMUs when defining limb movements while studying the model performance in clinical and laboratory settings.
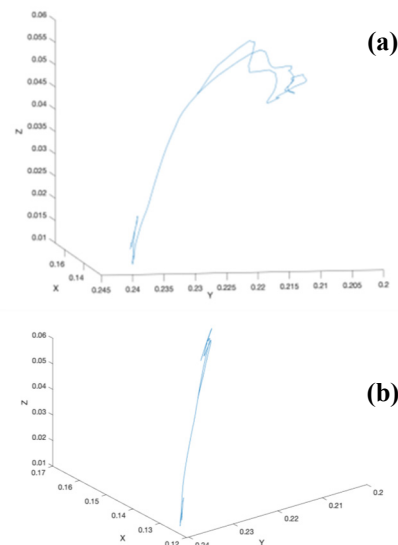

Figure 7: The elbow IAA trajectories as viewed at the oblique angle (a) and the sagittal plane containing the motion of flexion and extension (b). (units in meters, m).

By using the traditional optical-based motion tracking system, we have characterized the concept of a "knee axis" and further the concept of "invariant. (Kim & Vela, 2021; Kim, Veloso, Araújo, Vleck, & João, 2013)" We found that the line of the ground reaction force (GRF) vector is very close to the knee instantaneous axis (KIA). It aligns the knee joint with the GRF such that the reaction forces are torqueless. This insight shows that locating KIA is equivalent to the dynamic alignment measurement. This method can be used for the optimal design of braces and orthoses for the conservative treatment of knee osteoarthritis. Having validated the axis-angle with the optical-based system, we applied the same approach with the imu-based system to track the occupied motion of the subject.

The invariant combination of the axis-angle representation could open a new era of quantifying biomechanical perception-action systems as interactions with the natural or built environment. The overall performance metrics of many motor activities could be extended to real-world and clinical settings within multiple spatial and temporal frameworks. Further, this approach may then be extended to understanding the causal nature of biomechanical injury and disease, especially that associated with inertial kinetics and kinematics.

The kinesthesis, the awareness of one's own motion, cannot be measured in a sensor coordinate system (SCS.) However, they have unity relative to the posture and behavior of the subject being

considered. The results exert goal-directed feedback control by using the IAA to guide our motion continuously. Our assumption is that goal-directed feedback could be applied to many more rehabilitation application routines. Real-time posture correction and motion change instruction could ultimately optimize motor learning, reducing injuries caused by excessive motion and bad postures. Therefore, the shape of the IAA surface relative to the goal-directed behavior of the performer can be regarded as the "genome" of golf swing performance.

ACKNOWLEDGEMENTS

REFERENCES

Ancillao, A., Vochten, M., Verduyn, A., De Schutter, J., & Aertbeliën, E. (2022). An optimal method for calculating an average screw axis for a joint, with improved sensitivity to noise and providing an analysis of the dispersion of the instantaneous axes. *Plos one, 17*(10), e0275218.

Ball, R. (1900). *A Treatise on the Theory of Screws*: Cambridge University Press.

D'Amore, N., Ciarleglio, C., & Akin, D. L. (2015). *Imu-based Manipulator kinematic identification.* Paper presented at the 2015 IEEE International Conf. on robotics and automation (ICRA).

Gibson, J. J. (1979). *The Ecological Approach to Visual perception*: Houghton Mifflin.

González-Alonso, J., Oviedo-Pastor, D., Aguado, H. J., Díaz-Pernas, F. J., González-Ortega, D., & Martínez-Zarzuela, M. (2021). Custom IMU-based wearable system for robust 2.4 GHz wireless human body parts orientation tracking and 3D movement visualization on an avatar. *Sensors, 21*(19), 6642.

Kim, W. (2020). The Knee Proprioception as Patient-Dependent Outcome Measures within Surgical and Non-Surgical Interventions *Proprioception*: IntechOpen.

Kim, W., Araujo, D., Kohles, S. S., Kim, S.-G., & Alvarez Sanchez, H. H. (2020). Affordance-Based Surgical Design Methods Considering Biomechanical Artifacts. *Ecological Psychology*, 1-15. doi:10.1080/10407413. 2020.1792782

Kim, W., Kim, Y.-H., Veloso, A. P., & Kohles, S. S. (2013). Tracking knee joint functional axes through Tikhonov filtering and Plücker coordinates. *Journal of Novel Physiotherapies*(1).

Kim, W., Tretheway, D. C., & Kohles, S. S. (2009). An inverse method for predicting tissue-level mechanics from cellular mechanical input. *Journal of Biomechanics, 42*(3), 395-399.

Kim, W., & Vela, E. A. (2021). A Tensional Network in the Knee. *Biomedical Journal of Scientific & Technical Research, 40*(2), 32073-32078.

Kim, W., Veloso, A., Araújo, D., Machado, M., Vleck, V., Aguiar, L., .Vieira, F. (2013). Haptic perception-action coupling manifold of effective golf swing. *International Journal of Golf Science, 2*(1), 10-32.

Kim, W., Veloso, A. P., Araújo, D., Vleck, V., & João, F. (2013). An informational framework to predict reaction of constraints using a reciprocally connected knee model. *Computer Methods in Biomechanics and Biomedical Engineering*, 1-12. doi:10.1080/10255842. 2013.779682

Kuipers, J. B. (1999). *Quaternions and Rotation Sequences.* Princeton: Princeton University Press.

Lapresa, M., Tamantini, C., di Luzio, F. S., Ferlazzo, M., Sorrenti, G., Corpina, F., & Zollo, L. (2022). Validation of Magneto-Inertial Measurement Units for Upper-Limb Motion Analysis Through an Anthropomorphic Robot. *IEEE Sensors Journal, 22*(17), 16920-16928.

Schumacher, A. (2006). Integration of a gps aided strapdown inertial navigation system for land vehicles. *Master of Science Thesis, KTH Electrical Engineering.*

Teu, K. K., Kim, W., Fuss, F. K., & Tan, J. (2006). The analysis of golf swing as a kinematic chain using dual Euler angle algorithm. *Journal of Biomechanics, 39*(7), 1227-1238.

Tincknell, M. (2023). Quaternion. *MATLAB Central File Exchange.* Retrieved from https://www.mathworks. com/matlabcentral/fileexchange/33341-quaternion

Trujullo, D. M., & Busby, H. R. (1997). *Practical Inverse Anlaysis in Engineering*. Boca Raton: CRC Press.